The Zebrafish Annexin Gene Family

Steven A. Farber, Robert A. De Rose, Eric S. Olson, et al.

Genome Res. 2003 13: 1082-1096
Access the most recent version at doi:10.1101/gr.479603

Letter

The Zebrafish Annexin Gene Family

Steven A. Farber,[1,2] Robert A. De Rose,[1] Eric S. Olson, and Marnie E. Halpern

Department of Embryology, Carnegie Institution of Washington, Baltimore, Maryland 21210, USA

The Annexins (ANXs) are a family of calcium- and phospholipid-binding proteins that have been implicated in many cellular processes, including channel formation, membrane fusion, vesicle transport, and regulation of phospholipase A_2 activity. As a first step toward understanding in vivo function, we have cloned 11 zebrafish *anx* genes. Four genes (*anx1a*, *anx2a*, *anx5*, and anx11a) were identified by screening a zebrafish cDNA library with a *Xenopus anx2* fragment. For these genes, full-length cDNA sequences were used to cluster 212 EST sequences generated by the Zebrafish Genome Resources Project. The EST analysis revealed seven additional *anx* genes that were subsequently cloned. The genetic map positions of all 11 genes were determined by using a zebrafish radiation hybrid panel. Sequence and syntenic relationships between zebrafish and human genes indicate that the 11 genes represent orthologs of human *anx1,2,4,5,6,11,13*, and suggest that several zebrafish *anx* genes resulted from duplications that arose after divergence of the zebrafish and mammalian genomes. Zebrafish *anx* genes are expressed in a wide range of tissues during embryonic and larval stages. Analysis of the expression patterns of duplicated genes revealed both redundancy and divergence, with the most similar genes having almost identical tissue-specific patterns of expression and with less similar duplicates showing no overlap. The differences in gene expression of recently duplicated *anx* genes could explain why highly related paralogs were maintained in the genome and did not rapidly become pseudogenes.

Sequences of all zebrafish *anx* genes described in this paper have been deposited in GenBank. The accession nos. are as follows: *anx1a*, AY178793; *anx1b*, AY178794; *anx1c*, AY178795; *anx2a*, AY178796; *anx2b*, AY178797; *anx4*, AY178798; *anx5*, AY178799; *anx6*, AY178800; *anx11a*, AY178801; *anx11b*, AY178802; and *anx13*, AY178803.

Eleven Annexin (ANX) proteins have been identified in vertebrates (ANX1–7, 9, 11, 13, and 31). ANXs have also been identified in many other organisms, including plants (Smallwood et al. 1990a,b), *Hydra vulgaris* (Schlaepfer et al. 1992), *Dictyostelium discoideum* (Bonfils et al. 1994), *Giardia lamblia* (Fiedler and Simons 1995), *Caenorhabditis elegans* (Creutz et al. 1996), and *Drosophila melanogaster* (Johnston et al. 1990). The defining characteristics of all ANXs is that they share a highly conserved 70-amino acid domain that is repeated four to eight times, and they have the ability to bind anionic phospholipids in the presence of calcium (with the exception of ANX31, which lacks the calcium binding site; Moss 1992). The ANXs are the largest group of eukaryotic calcium-binding proteins that do not contain the E-F hand calcium-binding motif (Smith and Moss 1994). ANXs contain a highly divergent N-terminal domain that can vary from ten to hundreds of amino acids and is thought to confer unique functions to given family members (Fig. 1). Within the N-terminal domain of a number of ANXs, there are conserved tyrosine kinase (EGF receptor) and protein kinase C (PKC) sites that are phosphorylated during oncogenic transformation (Glenney Jr. 1985; de Coupade et al. 2000).

The function of this evolutionarily conserved family of proteins remains poorly understood. Studies on cultured cells suggest that ANXs function in a broad range of physiological processes (for a review, see Seaton 1996). For example, it has long been known that ANXs inhibit phospholipases in vitro (Huang et al. 1986; Davidson et al. 1987, 1990), and more recently, two ANXs (I and V) have been shown to inhibit phospholipase A2 in living cells (Kim et al. 1994; Croxtal et al. 1996). ANXs can also form volume-activated chloride currents (Nilius et al. 1996) and play a role in membrane fusion and vesicle transport (Bandorowicz-Pikula and Pikula 1998). During exocytosis, ANXs promote the aggregation of phospholipid membranes (Emans et al. 1993; Konig et al. 1998; Raynor et al. 1999), whereas arachidonic acid, which is released from membrane phospholipids by phospholipase A2 activity, promotes membrane fusion (Creutz 1981).

A number of studies have examined the evolutionary history of this gene family (Morgan and Fernandez 1997). Analyses of the gene structure of numerous ANXs have revealed a highly conserved intron–exon organization (for a review, see Smith and Moss 1994). Phylogenetic studies indicate that vertebrate ANX paralogs emanated from a common ancestor 800 million years ago and are now dispersed throughout the genome (Morgan and Fernandez 1997). The observation that ANXs are evolving at different rates suggests that paralogs have nonoverlapping functions (Morgan and Fernandez 1997; Morgan and Pilar Fernandez 1997; Morgan et al. 1999). The zebrafish (*Danio rerio*) genome has been subject to a round of duplication some 100–400 million years ago, after the divergence of fish and mammalian ancestors, resulting in an ~30% increase in the total number of genes (Postlethwait et al. 1999). Thus, the zebrafish provides the opportunity to examine why duplicated genes remain fixed in the genome as opposed to becoming pseudo genes.

This report describes the cloning and sequencing of zebrafish orthologs to vertebrate ANXs 1, 2, 4, 5, 6, 11, and 13. Expression of the *anx* genes during embryogenesis was examined by in situ hybridization not only to characterize each zebrafish ANX, but to compare the expression of recently du-

[1]Present address: Department of Microbiology and Immunology, Kimmel Cancer Center, Thomas Jefferson University, Philadelphia, PA 19107, USA.
[2]Corresponding author.
E-MAIL sfarber@lac.jci.tju.edu; FAX (215) 923-7144.
Article and publication are at http://www.genome.org/cgi/doi/10.1101/gr.479603.

13:1082–1096 ©2003 by Cold Spring Harbor Laboratory Press ISSN 1088-9051/03 $5.00; www.genome.org

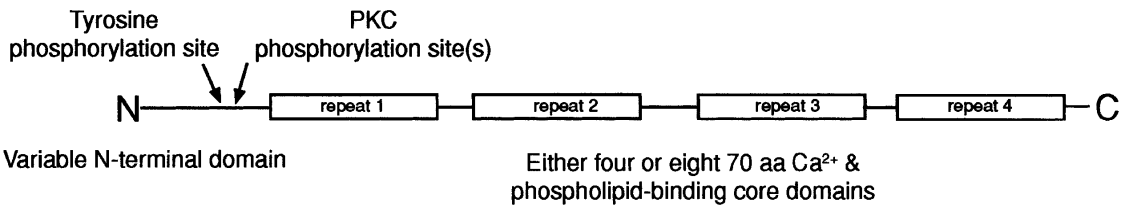

Figure 1 Canonical ANX structure. The N-terminal domains of ANX paralogs are highly variable, with the exception of highly conserved phosphorylation domains. At least two of the four ANX repeats are required to bind Ca^{2+} and phospholipid.

plicated gene paralogs. The nonoverlapping expression of duplicated genes suggests that the divergence of tissue specific functions drives the continued presence of ANX paralogs in the zebrafish genome.

RESULTS

Four zebrafish *anx* genes (*anx1a*, *anx2a*, *anx5*, and *anx11a*) were identified by low-stringency hybridization of a postsomite cDNA library by using a *Xenopus laevis anx2* probe. From comparisons with these genes, we identified seven additional *anx* genes by BLAST searches of zebrafish ESTs (see Table 1). Sequence alignments of the 11 zebrafish *anx* genes with mammalian *anx* genes revealed that three zebrafish *anx* genes were homologous with human *anx1*, two were homologous with human *anx2*, and two were homologous with human *anx11* (Fig. 2).

The predicted zebrafish ANX1b and ANX1c proteins are almost identical in their core repeat domain (97% identity in the first repeat), yet highly divergent in the N-terminal domain (33% identity). Only ANX1c contains the typical conserved EGF receptor and PKC phosphorylation sites observed in the N-terminal regions of mammalian ANX1 proteins (Fig. 2). Similarly, the predicted ANX2a and ANX2b proteins show higher identity in the repeat domain than in the N-terminal domain even though both paralogs contain the conserved N-terminal PKC phosphorylation site (Fig. 2). The ANX11 paralogs contain N termini rich in glycine, glutamine, and proline, characterized by a GYPPQPG repeat that is similar to that found in mammalian ANX11 proteins (Tokumitsu et al. 1992). As is the case for the other duplicated genes, the N-terminal regions of ANX11a and ANX11b are more divergent than are the repeat domains.

Despite the prevailing view that the N-terminal regions can be used to identify specific ANX family members, our analysis indicated that only the amino acids in the repeat domain were useful for phylogenetic analysis. With the exception of ANX4, all the zebrafish ANX N-terminal domains show little or no overall homology with their mammalian counterparts. For example, in the N-terminal region of ANX5, only the GTV motif is conserved between species (zebrafish, medaka, human, mouse, and chick), whereas most of the first repeat sequence is identical. The lack of homology in the N-terminal region of even closely related ANXs indicates that comparisons of this region would be less useful in elucidating the evolutionary relationships between fish ANXs. In contrast, the slow rate of mutation accumulation in the repeat region makes it useful for locating sequence similarities.

The phylogenetic tree of zebrafish, medaka (*Oryzias latipes*), pufferfish (*Fugu rubripes*), and human ANXs constructed by using only the amino acid sequence of the first ANX repeat reveals a close relationship between several pairs of duplicated zebrafish genes (Fig. 3). The *anx1b* and *anx1c* genes are the most closely related of all the duplicated paralogs. The phylogenetic analysis also suggests that we have identified orthologs to each of the four previously identified medaka ANXs. Medaka Max 1 is a likely ortholog of zebrafish ANX4, Max 2 is an ortholog of ANX5, Max 3 is an ortholog of ANX1, and Max 4 is an ortholog of ANX11.

To determine the timing of the duplication event observed in zebrafish, we searched the public databases for additional medaka *anx* sequences and identified 13 ESTs (data not shown). All but one of these new sequences cluster with the four previously published medaka *anx* genes (Max1 through Max4) already represented on the phylogenetic tree. The remaining clone was not a recent duplicate of these previously identified genes. Thus, the evolutionary relationship between the duplicated genes in these two species was not compared because of the paucity of medaka EST sequences. BLAST searches of fugu ESTs identified orthologs for zebrafish ANXs. Interestingly, phylogenetic analysis of these data (Fig. 3) suggests that fugu ANX1 and ANX2 paralogs were also duplicated, indicating that the duplication occurred in at least a subgroup of the Teleostei (Clupeocephala).

Syntenic Relationships Between Human and Zebrafish *anx* Genes

Because the N-terminal sequences of fish ANXs are considerably different from their mammalian counterparts, it is conceivable that zebrafish *anx* genes could be misidentified. To confirm that the 11 zebrafish *anx* genes were correctly assigned, we mapped the chromosomal position of each gene and, on the basis of the surrounding mapped genes, determined whether the given zebrafish *anx* gene showed conserved syntenies with its putative human ortholog. Ten of the 11 *anx* genes mapped to syntenic clusters containing the human ortholog (Fig. 4). For example, zebrafish *anx5* is surrounded by genes (*mel1ar*, *fga*, and *sc4mol*) that also map near the human *anx5* ortholog (Fig. 4D), indicating that the zebrafish gene was correctly identified.

The mapping data for the *anx1* genes indicate that all three genes lie on zebrafish linkage group (LG) 5. They probably arose by tandem duplication (Fig. 4A) because *anx1b* and *anx1c* map very close to each other (e.g., beyond the resolution of the radiation hybrid panel). Zebrafish *anx1c/anx1b* are closely linked to the zebrafish *trk* gene; this *anx1/trk* syntenic cluster is preserved in humans (Fig. 4A). Of the ANX1 proteins, only ANX1c has both the conserved tyrosine and threonine phosphorylation sites present in the human protein (Fig. 2), suggesting that *anx1c* is the most closely related to human *anx1*.

Mapping data for the *anx2* genes reveal the relationship between zebrafish and human chromosomes. The region containing *anx2a* is syntenic with a region of human chromosome 15 that contains *anx2* (Fig. 4C). However, both zebrafish

Table 1. Zebrafish Annexin ESTs

Clone	EST	Gene	Clone	EST	Gene	Clone	EST	Gene
fa01d11	AA495341	1a	fe15g04	AW128428	1a	fk86h09	BE201180	1a
fa01d11	AA495413	1a	fe16d06	AW116978	6	fk87c05	BE200562	1c
fa05d11	AA495031	1a	fe16d06	AW128478	6	fk87c05	BE201203	1c
fa05d11	AA495062	1a	fe23g04	AW059024	1*	fk87h08	BE200605	1a
fa16b09	AA606132	1b	fe36g11	AW117164	1a	fk87h08	BE201325	1a
fa22e03	AA605663	1c	fe36g11	AW128738	1a	fk89e04	BE200691	5
fa66e01	AA658724	2a	fe37d07	AW128288	5	fk89e04	BE201296	5
fa92b02	AI330716	11b	fe37d07	AW128788	5	fk93b10	BE556966	1a
fa93d04	AI331482	2a	fi08c10	AW128143	5	fk95a02	BE201562	2a
fa93d04	AI332090	2a	fi69d08	AW423191	5	fk96f12	BE201666	1a
fa93g02	AI331515	1b	fi73b04	AW343140	11a	fk97g09	BE201732	4
fa93g02	AI332162	1b	fi89f12	AW421306	3	fk97g09	BE557263	4
fa97e02	AI331333	1a	fi98b03	AW466704	*	fk98d10	BE201768	1a
fa97e02	AI332264	1a	fi98b03	AW510130	*	fk98d10	BE557304	1a
fa98e12	AI331304	2a	fj01c11	AW076603	4a	fk98f07	BE201783	5
fa98e12	AI331418	2a	fj01c11	AW077934	4a	fk98f07	BE557319	5
fa98f06	AI331309	5	fj01f04	AW076623	1b	fl02b05	BE201872	1a
fa98f06	AI331423	5	fj01f04	AW077961	1b	fl02b05	BE557344	1a
fa98g02	AI331316	1c	fj10f10	AW184217	5	fl04a05	BE201981	5
fa98g02	AI331430	1c	fj10f10	AW203168	5	fl04a05	BE557472	5
fb01d04	AI331722	2a	fj15f01	AW184537	11b	fl04b02	BE201987	1a
fb01d04	AI331746	2a	fj15f01	AW232190	11b	fl04b02	BE557480	1a
fb03b04	AI330831	1a	fj17g03	AW184689	1c	fl06f05	BE202117	1c
fb04a03	AI330976	11b	fj17g03	AW232322	1c	fl08c05	BE202212	2a
fb07f04	AI384320	5	fj20f05	AW202684	13	fl08c06	BE557634	2a
fb07g04	AI396958	5	fj21a04	AW202707	2a	fl09f01	BE557047	1a
fb09a08	AI396702	4a	fj26b07	AW232957	4a	fl09f01	BE605432	1a
fb09a08	AI397259	4a	fj38d12	AW280338	13	fl09f01	BE605432	1a
fb10b01	AI384973	1a	fj66c06	AW077764	2a	fl10e03	BE557775	1a
fb10b01	AI397327	1a	fj91c05	AW421433	13	fl10e03	BE605484	1a
fb10c06	AI384990	1b	fj94g06	AW421231	4a	fl10f08	BE557784	2a
fb11h07	AI384429	1b	fj94g06	AW422555	4a	fl10f08	BE605491	2a
fb11h07	AI384960	1b	fk02d05	AW566597	4	fl10h06	BE605504	2a
fb13c06	AI384226	5	fk03b10	AW566666	11a	fl11d06	BE557821	2a
fb13c06	AI396592	5	fk04d01	AW466773	2a	fl11g03	BE557846	1a
fb15d08	AI396641	1a	fk07c08	AW466818	4b	fl12f08	BE605559	1a
fb15d08	AI882710	1a	fk08h09	AW466394	1*	fl14f07	BE605642	2a
fb38g11	AI437194	1c	fk11a01	AW510237	2a	fl15c09	BE557930	1c
fb38g11	AI444361	1c	fk22f03	AW566900	1a	fl16b05	BE557967	1a
fb40a08	AI437290	13	fk23b02	AW566526	11b	fl16b05	BE605673	1a
fb40a08	AI461284	13	fk24a12	AW567284	1a	fl17d01	BE558015	1a
fb40h01	AI444277	1b	fk24a12	AW594790	1a	fl17d05	BE558019	2a
fb40h03	AI461328	1b	fk26b11	AW567479	2a	fl19g08	BE558121	2a
fb52b02	AI476872	2b	fk29a06	AW567545	4	fl19g08	BE605746	2a
fb57f04	AI477453	2b	fk29a06	AW595172	4	fl20d09	BE558162	1a
fb59b10	AW018621	2b	fk31e12	AW566920	2a	fl20d09	BE605780	1a
fb60g02	AI497488	11b	fk31e12	AW595499	2a	fl20f01	BE558169	1a
fb65e04	AI545799	4a	fk36g03	AW595256	2a	fl20f01	BE605793	1a
fb65e10	AI544742	4a	fk40a05	AW778666	1a	flo8c06	BE202113	2a
fb69d06	AI544877	11a	fk65d07	BE016101	1a	fm75d10	BF938344	13
fb69d06	AI544926	11a	fk65d07	BE016572	1a	fm79e05	BF938645	5
fb71b11	AI545200	4a	fk65f01	BE016703	2a	fm95g05	BG799346	1a
fb92c11	AI584862	11b	fk68a10	BE016198	1a	fm96h08	BG799431	1a
fc09a11	AI601281	11a	fk68a10	BE016726	1a	fp23c12	BG883870	11a
fc09a11	AI629060	11a	fk68f07	BE016228	2a	fp66e04	BG739067	11b
fc20a07	AI658201	5	fk68f07	BE016768	2a	fq90g12	BG892099	2a
fc44g02	AI794466	2a	fk69h01	BE016364	1a	fq92c05	BG892182	1a
fc44g02	AI883271	2a	fk69h01	BE016847	1a	fq92d07	BG892191	1a
fc63e05	AI883404	13	fk70a12	BE016380	1a	RZBAA36	AI964147	11a
fc65c09	AI878734	2a	fk70a12	BE016865	1a	RZBAA36	AI964148	11a
fc65c09	AI883512	2a	fk71a08	BE016928	1c	zeh0376	AI353349	11b
fc65f07	AI883535	11b	fk72h02	BE016998	5	zehl0196	AW453608	5
fc87g05	AI943258	2a	fk75a05	BE017050	1a	zehl1082	AW453598	1c
fc87g06	AI965162	2a	fk75a05	BE017357	1a	zehl2341	AW454928	11b
fc94h04	AI957567	11b	fk75a10	BE017362	1a	zehn0184	AI616512	4a
fc94h04	AI958668	11b	fk77d05	BE017181	1a	zehn0306	AI618466	1b
fd25c12	AI959209	11a	fk81a02	BE017610	2a	zehn1052	AI617080	2a
fd48f04	AW018574	4a	fk81g06	BE017653	1a	zehn1601	AI617459	11b
fd54h03	BF717976	3	fk84d04	BE200977	2a	zehn2370	AI617967	2b
fd59g04	AW018667	11b	fk84f04	BE200999	1a	zewp0221	AI618675	1a
fd59g04	AW019090	11b	fk86h09	BE017946	1a			

Two hundred twelve ESTs were identified by alignment with cloned zebrafish annexins as of July 15, 2001.
*indicates poor quality sequence that prevented paralog assignment.

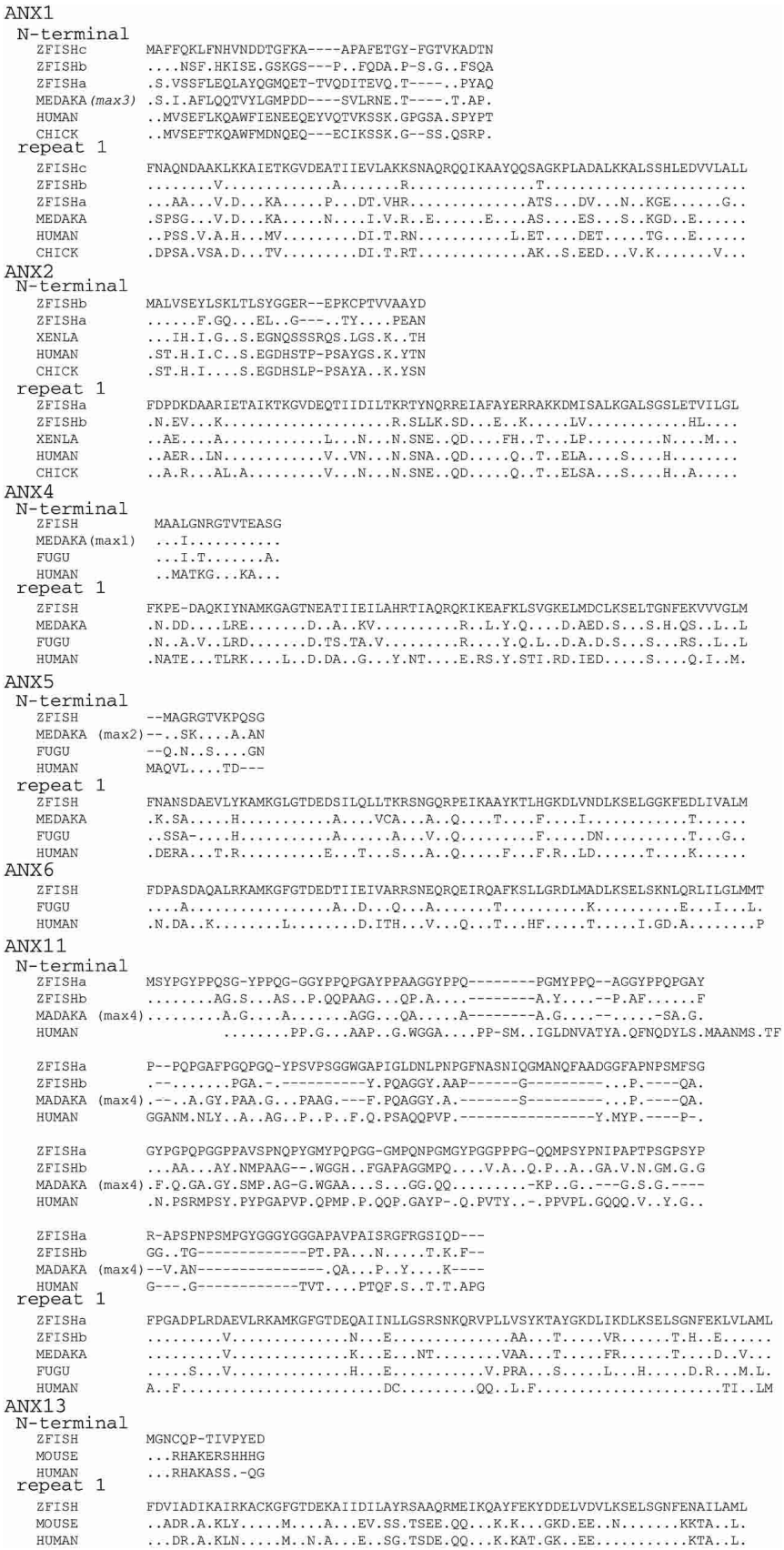

Figure 2 Comparisons of zebrafish ANX amino acid sequences. The corresponding proteins were aligned by using CLUSTALW, revealing significant divergence in their N-terminal domains as opposed to the first core repeat.

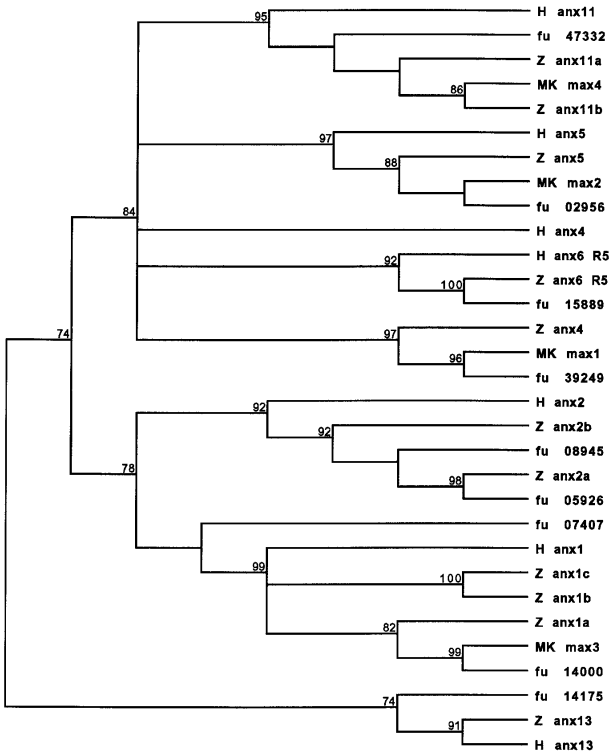

Figure 3 Phylogenetic relationships of the human, zebrafish, pufferfish (*Fugu rubripes*), and medaka (*Oryzias latipes*) ANXs. Medaka ANX sequences were obtained from GenBank: max1, CAA72125; max2, CAA72123; max3, CAA72124; max4, CAA72122.

anx2 genes are surrounded by orthologous genes that map to either human chromosome 11 or 15, suggesting that these clusters of human genes once resided on a single ancestral chromosome that split after divergence of mammalian and zebrafish genomes. The mapping results for zebrafish *anx11* genes are more clear-cut, indicating that both paralogs are surrounded by genes with human orthologs that map to the same region on human chromosome 10 (Fig. 4F). These mapping results unequivocally relate mammalian *anx* genes to those found in zebrafish.

Expression of Zebrafish Genes

The temporal expression patterns of zebrafish *anx* genes were examined by whole-mount in situ hybridization and, in some instances, validated by Northern analysis. The three *anx1* genes are primarily expressed in the outermost embryonic cells, known as the enveloping layer (Kimmel et al. 1995), during the period (~4 to 9 h postfertilization [hpf]) when this layer is dividing and migrating over the large yolk cell in a process termed epiboly (Fig. 5A–C). After epiboly is completed and somatogenesis begins, the expression of all three *anx1* genes is reduced, as exemplified by expression of *anx1a* at the midsomite stage (Fig. 5D) and by Northern analysis (Fig. 5K). By 24 hpf, *anx1* transcripts increased primarily in the outer ectoderm, with the expression level of *anx1a* being the highest (Fig. 5E). It is only at this stage that divergence between the paralogous *anx1* genes is observed. Not only is the expression of *anx1b* and *anx1c* reduced compared with *anx1a*, but *anx1c* is selectively expressed in a small group of cells close to the yolk and posterior to the eyes (Fig. 5F,G). After 80 hpf, all three *anx* genes were expressed in gill arches, epithelium, and fin buds (Fig. 5H,I), but only *anx1a* was expressed in the cells surrounding the swim bladder (Fig. 5I).

The zebrafish *anx2* gene paralogs are significantly more divergent in their core domain as compared with *anx1b* and *anx1c* paralogs (76% versus 94%; Fig. 2). We also found that the zebrafish *anx2* paralogs do not exhibit overlap in their expression patterns (Fig. 6). *anx2a* was expressed in the notochord (Fig. 6A) and in a subset of enveloping layer cells (Fig. 6B). Notochord expression was detected at the end of epiboly through early somite stages (Fig. 6C,D), and decreased in an anterior to posterior fashion. By the 21-somite stage, *anx2a* expression was observed only in the caudal-most notochord (Fig. 6E) and, after 24 hpf, in the epithelium and cells around the anus (Fig. 6F). In contrast, *anx2b* expression was not observed during early embryonic development (data not shown) and was first detected at ~48 to 80 hpf in the cells of the intestinal epithelium (Fig. 6G). Transcripts were observed in both the proximal (Fig. 6H) and distal segments of the differentiating intestine (Fig. 6I).

The zebrafish *anx4* ortholog was expressed during the onset of somatogenesis in the floor plate and in two lateral stripes (Fig. 7A) that most likely correspond to the pronephric duct precursor cells (Drummond et al. 1998). Two-color in situ hybridization with *anx4* and *draculin*, a marker of blood cell precursors (Herbomel et al. 1999), confirmed that the lateral *anx4*-expressing cells were not hematopoietic precursors (Fig. 7F,G). At the 21-somite stage, *anx4* is predominately expressed in floor plate, hypochord, and pronephros (Fig. 7B), a pattern that continues through 24 hpf (Fig. 7C,H). Additionally, at 24 hpf, expression was observed in the otolith, glomerulus, pronephric tubules, and pronephric ducts (Fig. 7D). Tissue-specific *anx4* expression was assigned on the basis of its similarity with *pax2*, a previously established marker of pronephros development (Drummond et al. 1998), which also labels these structures. After 70–80 hpf, *anx4* was expressed predominantly in the liver and gall bladder (Fig. 7I,J). The expression of *anx4* in the pronephros is consistent with its reported role in regulating Cl^- conductance in fluid secreting epithelia (Kaetzel et al. 1994).

Zebrafish *anx5* showed the most restricted pattern of expression during embryonic development. During somatogenesis, transcripts were found in the blood islands (21 somites, Fig. 8A) and at the most anterior tip of the embryo (26 somites; Fig. 8B). Cells in the olfactory placodes also expressed *anx5* (Fig. 8C). At 24 hpf, expression was mostly restricted to the olfactory placodes, hatching gland cells, and anus (Fig. 8D). After 80 hpf, expression was maintained in the developing nasal epithelium and in the anus; cells surrounding the swim bladder also expressed *anx5*. After 120 hpf, the cells surrounding the opening to the mouth expressed *anx5* (Fig. 8E), suggesting that these cells were related to the *anx5*-expressing cells observed in the anterior most region at the 26-somite stage (data not shown). Consistent with the RNA in situ gene expression data, Northern analysis of *anx5* transcripts revealed a 2.2-kb message that was initially detected at the 22-somite stage (Fig. 8F). Expression was also detected in RNA from 256 cell embryos, a stage prior to the onset of zygotic transcription, indicating some maternal contribution of *anx5* RNA to the embryo.

anx11a expression was observed at the end of gastrulation predominantly in the notochord (Fig. 9A,B). Unlike *anx2a*, which was also expressed in the developing notochord, there was no enveloping layer expression. As somato-

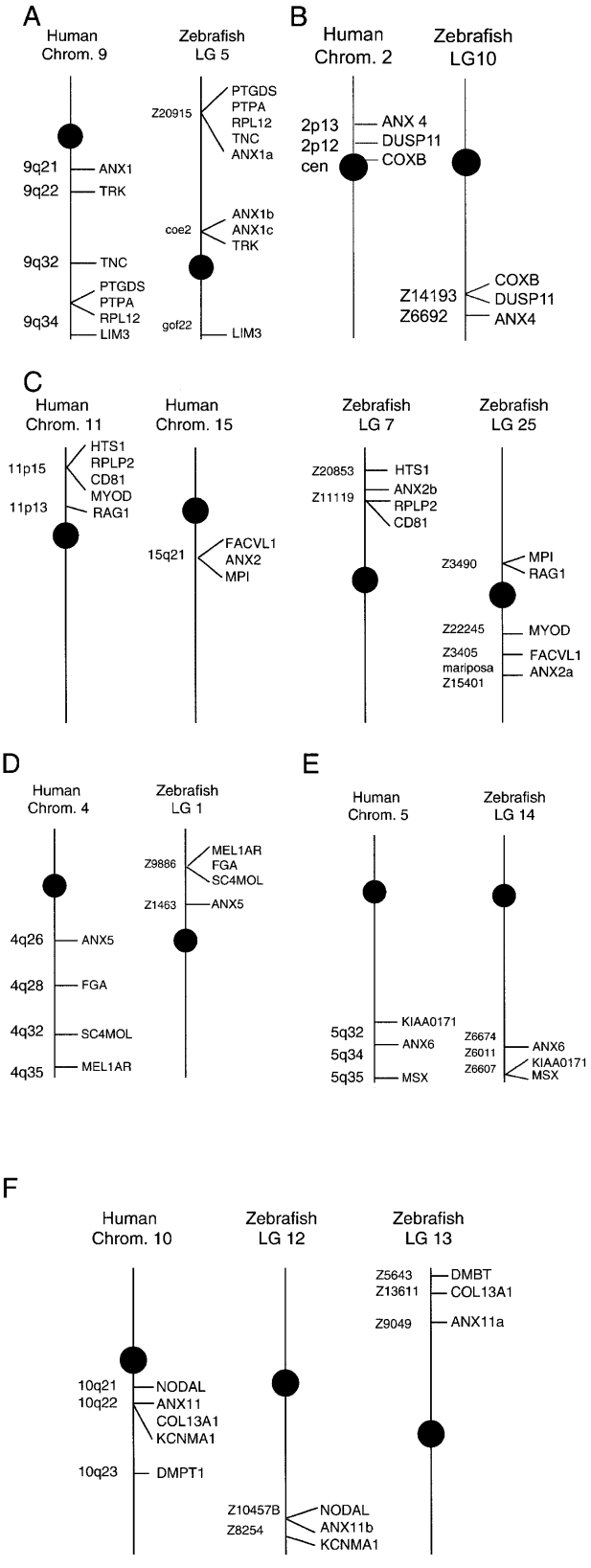

Figure 4 Map positions of human and zebrafish gene orthologs.

genesis advanced, expression was seen to shift from the axial mesoderm to the adaxial mesoderm (cells directly adjacent to the notochord; Fig. 9C). It was previously shown that in the absence of notochord, there is decreased adaxial expression of MyoD, a transcription factor that is known to play a role in myogenesis (Weinberg et al. 1996). To test whether differentiated notochord was similarly required for the adaxial expression of *anx11a*, *no tail* embryos, which are known to lack notochord (Halpern et al. 1993), were examined. The transition of *anx11a* expression to adaxial cells was unaffected in *no tail* embryos (Fig. 9D). In wild-type embryos, the shift in expression away from the midline to more lateral structures continued as development proceeded, such that by 24 hpf, expression was observed in the paraxial mesoderm, anus, and periderm (Fig. 9E,F). The *anx11a* paralog, *anx11b*, was only weakly detected in the notochord of four-somite embryos (data not shown); however, at 24 hpf, *anx11b* showed strong expression in the periderm similar to *anx11a* (Fig. 9F). Later in development, *anx11a* was expressed more intensely in the liver (arrowhead) than in the intestine (arrow; Fig. 9G), the opposite to the expression pattern of *anx11b* (Fig. 9H). Northern analysis of *anx11a* expression revealed a 2.2-kb message that was detected from the end of gastrulation to the adult stage (Fig. 9I).

The *anx6* gene was primarily expressed in somitic mesoderm from the midsomite stages (Fig. 10A) to 24 hpf (Fig. 10B,C). Little expression was detected after 72 hpf (data not shown). *anx13* is detected during gastrulation in the notochord and in an area at the anterior-most portion of the embryo in a region called the polster (Fig. 10D,E). At the 21-somite stage, *anx13* expression was maintained in the notochord and central nervous system (CNS; Fig. 10F,G). After 24 hpf, expression persisted in much of the CNS (retina, floor plate, etc.) and nonsomitic mesoderm (Fig. 10H,I). At later stages, *anx13* was expressed throughout the embryo (data not shown), being the most widely expressed of all the *anx* genes.

DISCUSSION

The ANXs comprise a family of Ca^{2+} and phospholipid binding proteins that contain four or eight highly conserved repeating domains of ~70 amino acids (Seaton 1996). Data largely from cell culture studies indicate that ANXs are regulated by growth factor–mediated tyrosine phosphorylation (Brugge 1986; Huang et al. 1986) and by PKC phosphorylation (Schlaepfer et al. 1992; Minin et al. 1998; Schmitz-Peiffer et al. 1998). ANXs can inhibit phospholipase A_2 activity (Brugge 1986; Huang et al. 1986; Kim et al. 1994; Croxtal et al. 1996; Mira et al. 1997), form channels (Nilius et al. 1996), and regulate membrane trafficking (Donnelly and Moss 1997; Gerke and Moss 1997; Bandorowicz-Pikula and Pikula 1998; Kobayashi et al. 1998). It is likely ANXs play key roles in regulating a variety of signal transduction events. ANXs are also ubiquitous in eukaryotic cells and can represent ≥1% of total cell protein (Seaton 1996). Although there is now a body of literature describing the interesting properties of ANXs, their in vivo functions remain elusive.

As a first step toward exploring the function and evolution of the vertebrate *anx* gene family, we cloned 11 zebrafish *anx* genes by cDNA library screening and the analysis of zebrafish ESTs deposited in GenBank. In studying ANX evolution, the zebrafish has the advantage that there was a genome-wide duplication some 100 million years ago, well after fish and mammals diverged, followed by selective

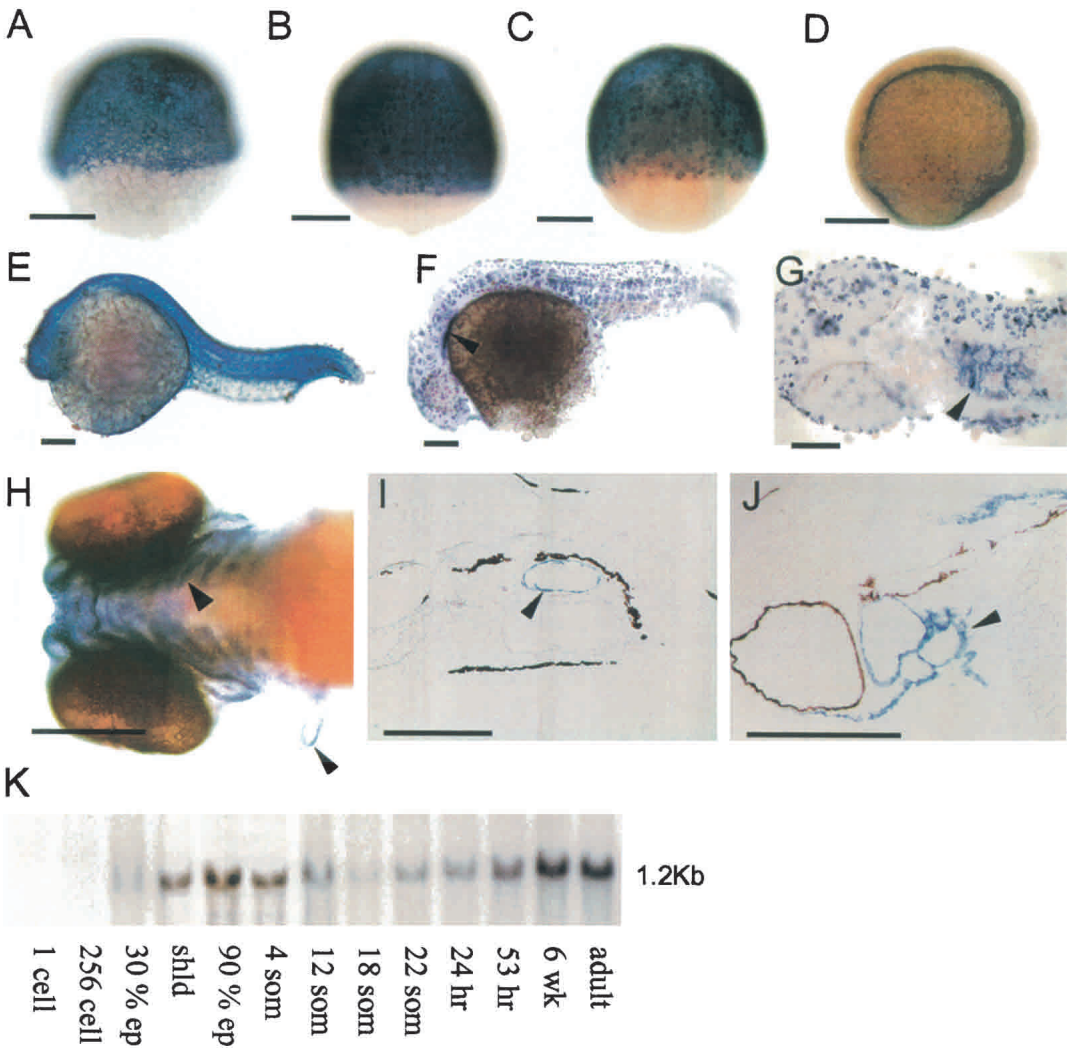

Figure 5 Expression of *anx1* paralogs. (*A–C*) Lateral views of 70% epiboly stage embryos revealing enveloping layer expression of *anx1a* (*A*), *anx1b* (*B*), and *anx1b* (*C*). (*D*) *anx1a* expression is markedly reduced by the 12-somite stage and then reappears in the periderm (*E*) at 24 hpf. (*F*) Periderm expression of *anx1c* at 24 hpf. *Arrowhead* indicates a domain of *anx1c* expression not found with *anx1a* and *anx1b*. (*G*) A higher magnification dorsal view of the *anx1c* unique expression domain. A ventral view (*H*) and sagittal section (*I*) of 80-hpf embryos showing *anx1a* expression in the gills, epithelium, fin buds, and the cells of the swim bladder (*arrowhead*). (*J*) At 80 hpf, *anx1c* was expressed predominately in the epithelium. (*K*) Embryonic and adult expression of *anx1a* determined by Northern analysis. Total RNA was isolated from zebrafish embryos at selected stages from the one-cell stage to adult. Scale bar, 200 μm.

gene loss (Postlethwait et al. 1999). Thus, it is possible to study how sibling paralogs diverged in both sequence and expression.

Phylogenetic and BLAST analysis of the 11 *anx* genes indicated that zebrafish contain three paralogs of *anx1*, and duplicates of *anx2* and *anx11* (Figs. 2, 3). The prevailing view based on the study of mammalian *anx* genes is that the N-terminal variable domain acts as a "fingerprint" to identify ANX family members (Moss 1992). The zebrafish data do not support this idea because the N-terminal domains have diverged so considerably that they were of little use in determining the correct ortholog (data not shown). This was in contrast to comparisons using the repeat domain. Once zebrafish genes were assigned to a particular ANX subtype, CLUSTAL alignments of the N-terminal domains with mammalian orthologs often revealed the conservation of key phosphorylation sites. In fact, the only recognizable homology in the N-terminal regions was in amino acids surrounding well-established regulatory domains important for phosphorylation.

To confirm that we had correctly identified a given zebrafish ANX, we localized each gene to the zebrafish genetic map. We were able to establish the identities of 10 of the 11 zebrafish genes by their position within syntenic gene clusters (Fig. 4). Four previously described medaka genes (*max1*, *max2*, *max3*, and *max4*) were also included in our phylogenetic comparisons. Sequence analysis indicated that medaka ortholog *max3* corresponds to zebrafish *anx1a*, *max1* to *anx4*, *max2* to *anx5*, and *max4* to *anx11b*. Osterloh et al. (1998) observed the variability in the N-terminal portion of the medaka proteins and concluded that *max3* and *max4* were "novel" ANX family members. However, the zebrafish data clearly illustrates that *anx11b* (*max4*) maps to a region syntenic with human *anx11*. Similarly, the synteny data also reveals that *max1* and *max2*

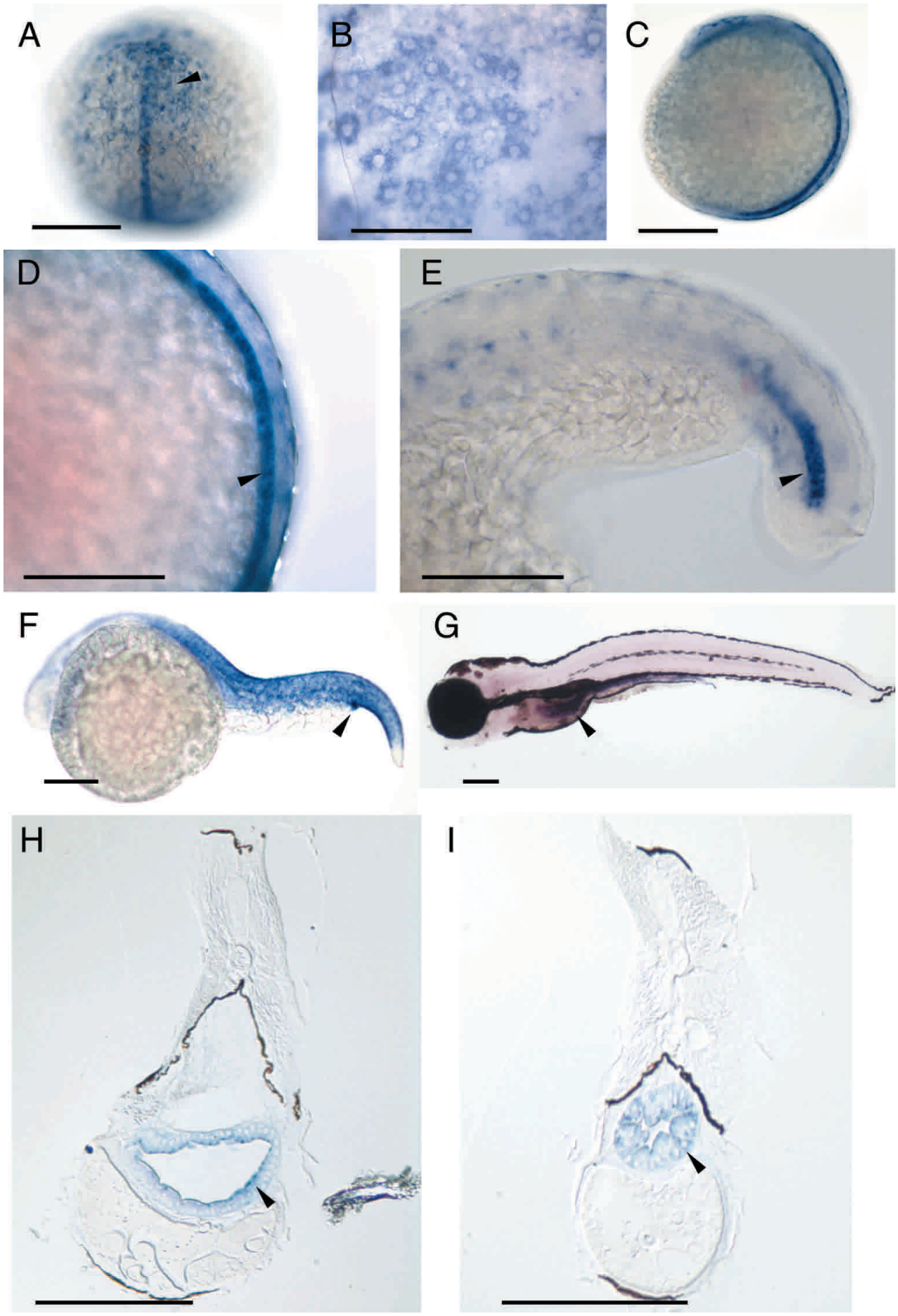

Figure 6 Expression of *anx2* genes. (*A*) Dorsal view of a 100% epiboly stage embryo revealing both notochord and enveloping layer expression (*arrowhead*) of *anx2a*. (*B*) Higher magnification view of embryo in *A*, highlighting enveloping layer expression. (*C*) A lateral view of notochord expression of *anx2a* throughout the entire anterior to posterior axis; (*D*) a higher power lateral view of the same embryo. (*E*) A lateral view of a 21-somite embryo with only posterior *anx2a* expression remaining. (*F*) At 24 hpf, *anx2a* expression is predominately in the periderm not notochord and then later in the skin (data not shown). (*G*) *anx2b* expression in the intestine at 72 hpf (*arrowhead*). Sagittal sections through both the proximal (*H*) and distal (*I*) intestine indicate *anx2b* expression in the apical brush border of the intestinal epithelium (*arrowhead*).

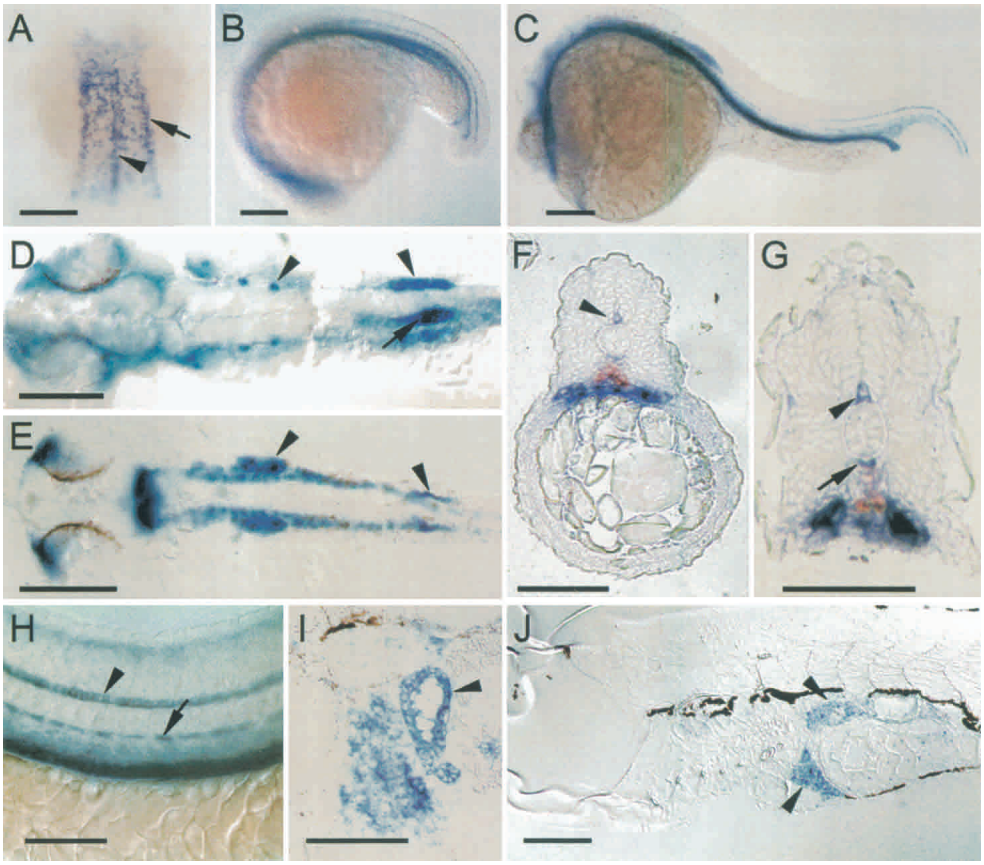

Figure 7 Expression of *anx4*. (*A*) Dorsal view of a four-somite embryo revealing *anx4* transcripts in the floor plate (*arrowhead*) and in two lateral stripes (*arrow*) corresponding to pronephric duct precursor cells. Lateral views of a 21-somite (*B*) and a 24-hpf (*C*) embryo with prominent *anx4* expression in the floor plate, hypochord, and pronephros. (*D*) Dorsal view at 24 hpf also shows *anx4* expression in the otolith, glomerulus (midline arrowhead), pronephric tubulues, and pronephric ducts. (*E*) A similar dorsal view illustrating *pax2* transcripts in the otolith, pronephric tubulues, and pronephric ducts but not the glomerulus. Hematopoietic precursors were simultaneously visualized in cross sections using one riboprobe for *draculin* transcripts (red) and another for *anx4* transcripts (blue) at both the 20-somite (*F*) and (*G*) 24-hpf stages. (*H*) A lateral view at 24 hpf also localizes *anx4* expression to floor plate (*arrowhead*), hypochord (*arrow*), and pronephros. Cross sections of 3-hpf larvae reveal *anx4* expression predominately in the gall bladder (*I*) and liver (*J*). (*A–E*) Bar, 200 μm; (*F–J*) bar, 100 μm.

are orthologs of human *anx4* and *anx5*, respectively. From these findings, a strong argument can be made that sequence comparisons need to be coupled with gene mapping and synteny data to understand the evolution of a complex multigene family such as the ANXs.

Increases in ploidy have been found for many cypriniform fish (Aparicio 1998), a group that includes the zebrafish. Although the zebrafish is diploid, its genome has retained ~30% of the duplicated genes that occurred after fish and mammalian ancestors diverged, even though these genes were initially redundant (Amores et al. 1998; Postlethwait et al. 1998; Prince et al. 1998; Force et al. 1999). It is expected that, following duplication, redundant genes accumulate mutations that would rapidly transform one of the gene paralogs into a nonfunctional pseudogene. Although this certainly occurs in many cases, the rate of gene silencing is often much less than predicted by a number of genetic models (Meyer and Schartl 1999). The duplication-degeneration-complementation (DDC) model has been proposed to explain the retention of duplicated genes (Force et al. 1999). This model considers the effect of mutations in noncoding regions, and predicts that if duplicate genes accumulate mutations in regulatory elements, then their expression might no longer overlap. Once expression between recently duplicated gene paralogs is nonredundant, it is more likely that the activity of both genes is now required to maintain the function of the single ancestral ortholog. Wagner (2000) suggests an alternative view that genes with overlapping or partially redundant functions might be maintained to offer protection from deleterious mutations. If one applies such models, then duplicated gene paralogs should have nonoverlapping aspects of their expression, and the combined expression patterns of recently duplicated paralogs should be consistent with the expression of a single mammalian ortholog.

Given the high degree of nucleotide identity and their proximity in the genome, *anx1b* and *anx1c* most likely arose from a single gene that was subject to a more recent tandem duplication event (Fig. 4A). Even though these paralogs are 94% identical in the first repeat, they have diverged extensively in their N-terminal domains (Fig. 2). This pattern was true for the other duplicated genes as well. Smith and Moss (1994) have argued that because these domains are "unique," they likely mediate the specific functions of each *anx* gene. If the accepted view that the ANX N-terminal domains defines ANX function holds, then these duplicated paralogs have evolved very different functions. Whether this hypothesis is

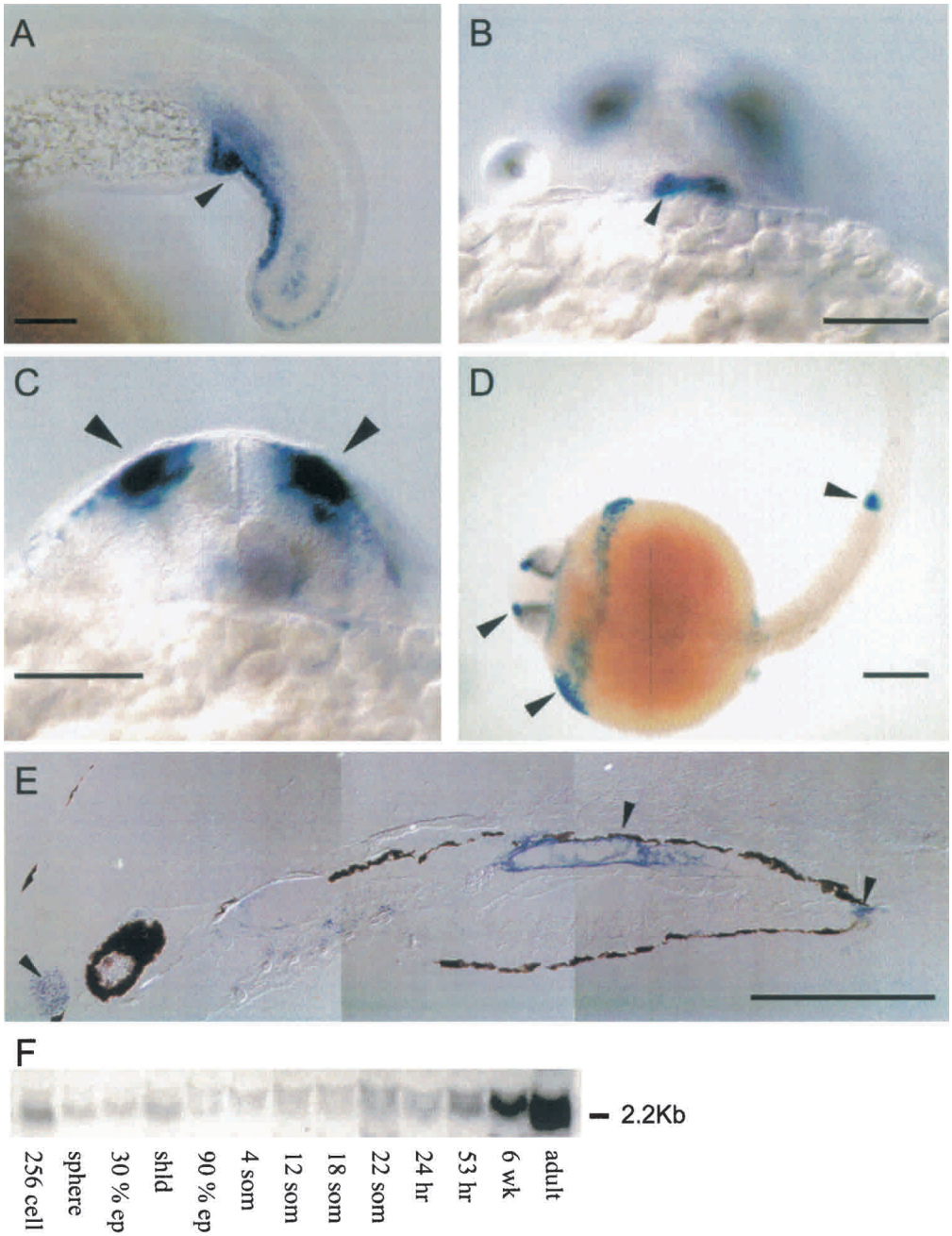

Figure 8 Expression of *anx5*. (*A*) Lateral view of a 21-somite embryo revealing *anx5* transcripts in blood island (*arrowhead*). Coronal view of a 26-somite embryo indicates *anx5* expression in the most anterior domain (*B*) and in the olfactory placodes (*C*). (*D*) Ventral view of a 24-hpf embryo reveals intense *anx5* expression in the olfactory placodes, hatching gland cells, and anus. (*E*) Sagittal section through an 80-hpf larvae reveals expression in the developing nasal epithelium, anus, and swim bladder. (*F*) Embryonic and adult expression of *anx5* determined by Northern analysis. Total RNA was isolated from zebrafish embryos at selected stages from the one-cell stage to adult. (*A–C*) Bar, 100 μm; (*D, E*) bar, 200 μm.

correct must await direct functional analysis of the sibling genes.

An analysis of the three zebrafish *anx1* genes revealed that the ancestral *anx1* gene common to both fish and mammals was duplicated most likely as a result of the predicted genome duplication event >100 million years ago. This resulted in *anx1a* near Z20915 and a second *anx1* gene near marker *coe2*. This second *anx1* gene was more recently duplicated to yield an additional *anx* gene at the *coe2* locus as evidenced by the high degree of sequence homology between *anx1b* and *anx1c* paralogs (Figs. 2A, 4A). Early in development, gene expression of all three *anx1* paralogs was largely overlapping; however, by 24 hpf, differences emerged. Only *anx1c* was expressed in the anterior domain near the eyes and close to the yolk. However, it is possible that there are significant differences in expression levels of each *anx1*

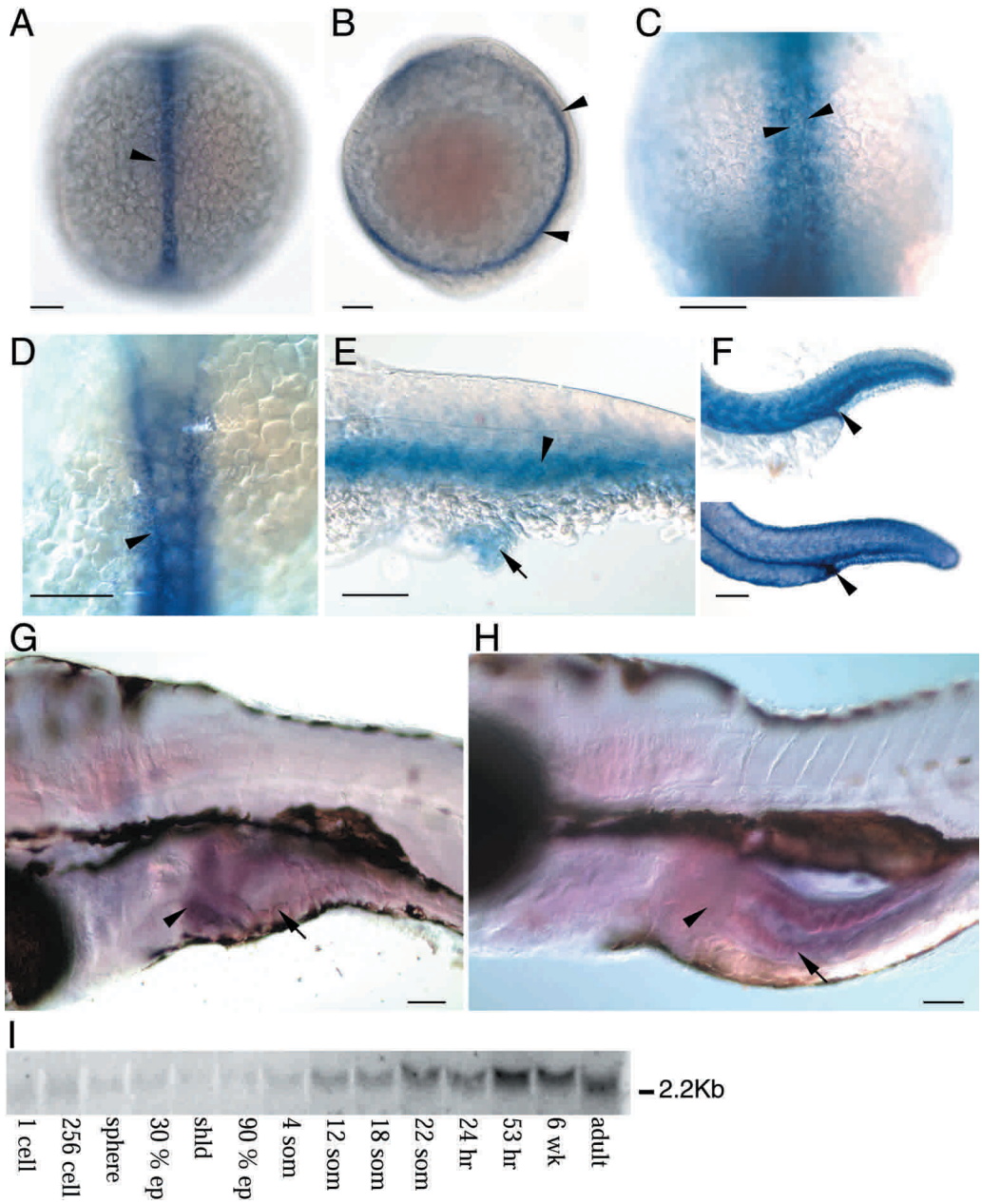

Figure 9 Expression of *anx11* genes. Dorsal (*A*) and lateral (*B*) views of notochord *anx11a* expression in a four-somite embryo. (*C, D*) Dorsal views of 15-somite embryos illustrating a shift in *anx11a* expression from the axial mesoderm to the adaxial mesoderm that is also observed in embryos that lack differentiated notochord (*D*; *no tail*$^{-/-}$). (*E*) By 24 hpf, *anx11a* expression was observed in the paraxial mesoderm (*arrowhead*) and anus (*arrow*). (*F*) Lateral views of 24-hpf embryos reveal expression of both *anx11a* (*top*) and *anx11b* (*bottom*) in the periderm, *arrowhead* marks the anus. (*G, H*) Lateral views of 80-hpf larvae indicating greater levels of *anx11a* transcripts (*G*) in the liver (*arrowhead*) than that of *anx11b* (*H*). Embryonic and adult expression of *anx11a* determined by Northern analysis. (*I*) Total RNA was isolated from zebrafish embryos at selected stages from the one-cell stage to adult. Bar, 100 μm.

ortholog (as suggested by the time needed for staining; data not shown), something that can be more accurately quantified in further studies using quantitative reverse transcription–polymerase chain reaction (RT-PCR).

The overlap in expression of the *anx2* paralogs was significantly different from that observed for the *anx1* genes. The *anx2* paralogs had no detectable overlap in expression, in that *anx2b* transcripts were not detected until the onset of intestinal development (48 hpf), whereas *anx2a* was expressed during gastrulation in the notochord and later in the periderm (Fig. 6). Given that mammalian *anx2* is expressed in both the skin and intestinal epithelium (Bastian et al. 1993; Ma and Ozers 1996; Munz et al. 1997; Dreier et al. 1998; Massey et al. 1998), it is likely that the expression of both zebrafish *anx2* paralogs is required to provide the equivalent function of the human ortholog. Consistent with its selective role in intestinal physiology, preliminary data indicate that disruption of *anx2b* translation by antisense injections at the one-cell stage

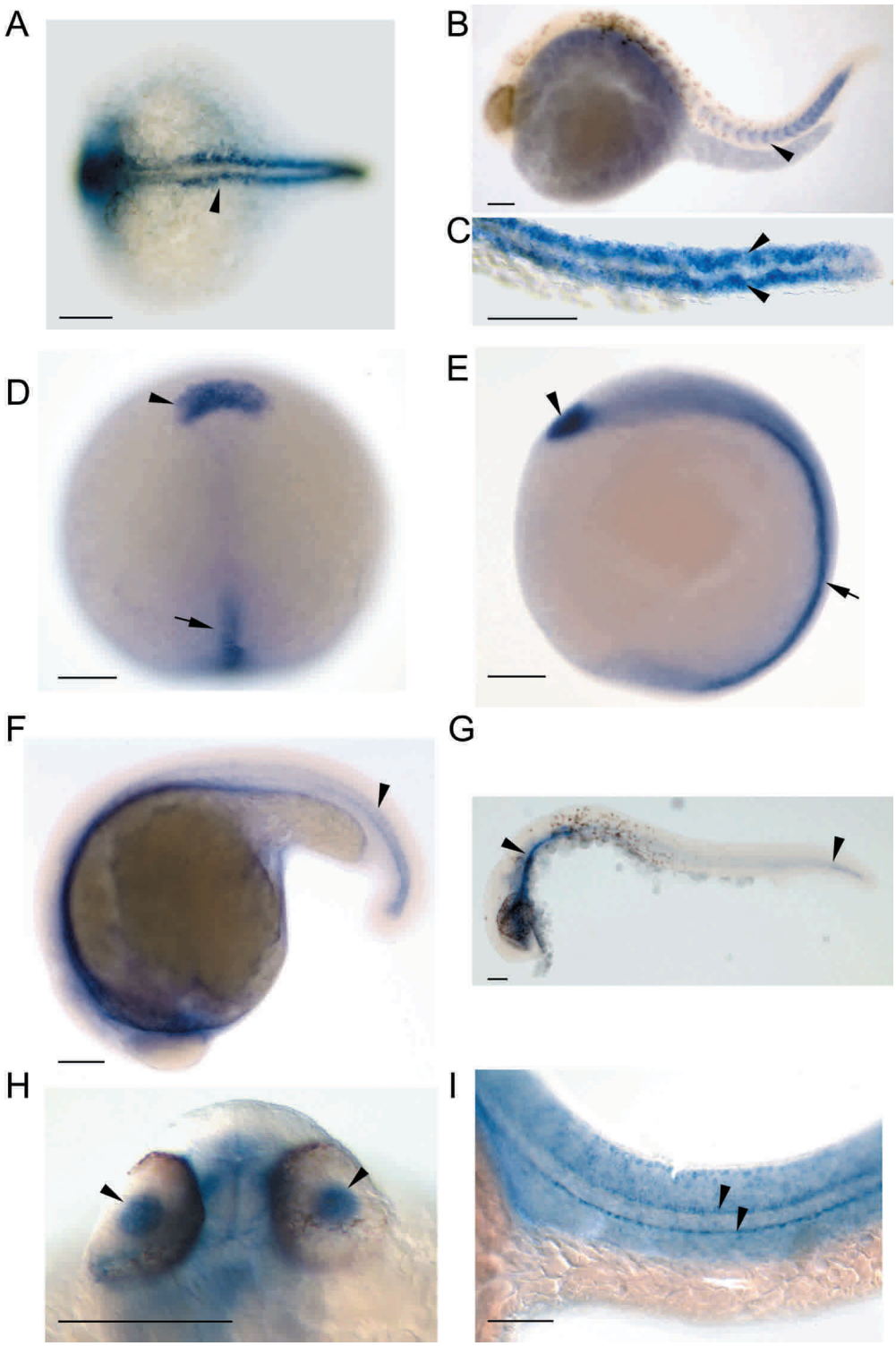

Figure 10 Expression of *anx6* and *anx13* genes. (*A*) Dorsal view of an 18-somite embryo reveals *anx6* expression in somitic mesoderm. This pattern of *anx6* expression continues through to 24 hpf, lateral view (*B*) and dorsal view (*C*). Dorsal (*D*) and lateral (*E*) views of *anx13* expression in both the notochord (*arrow*) and polster (*arrowhead*) of bud stage embryos. Lateral views of 21-somite (*F*) and 24-hpf (*G*) embryos reveal that *anx13* expression is maintained in the notochord and expands to the CNS. (*H*) Dorsal view at 24 hpf indicates *anx13* expression in the retina (*arrowhead*). (*I*) Lateral view of the tail at this stage indicates notochord, floor plate, and nonsomitic mesoderm. Bar, 100 μm.

profoundly affects cholesterol uptake, whereas disruption of *anx2a* does not (E. Smart, R. DeRose, and S. Farber, in prep.). A major effort to identify the specific amino acids mediating this effect is underway by examining the differences between the two zebrafish ANX2 paralogs identified in this study and by comparison to murine ANX2.

As was the case with *anx2*, *anx11* paralogs exhibited significant differences in expression. Only *anx11a* was expressed during gastrulation (notochord) and somatogenesis (adaxial and paraxial mesoderm), whereas periderm expression was observed for both paralogs at 24 hpf (Fig. 9A–F) After 80 hpf, *anx11a* was expressed more intensely in liver, whereas *anx11b* was greater in intestine (Fig. 9G,H). The observation that duplicated zebrafish genes often have nonoverlapping expression patterns was also observed in a recent study of Na, K-ATPases (Rajarao et al. 2001).

The observation that the evolutionary divergence between *anx2* paralogs is clearly greater than that observed between *anx1b* and *anx1c* paralogs not only indicates that the *anx1* gene duplication was a more recent event but illustrates how gene paralogs evolve. These studies have enabled us to focus our efforts on elucidating the function of both ANX2 and ANX4. Interestingly, ANX4 is expressed in the identical tissues (floor plate and kidney) of both zebrafish and mouse, in which analysis of the "knock out" phenotype is underway (J. Dedman, pers. comm.). Work is ongoing to compare the phenotypes observed with zebrafish ANX4 "morphants" with those observed in the mouse knock outs. With the availability of antisense techniques for the zebrafish, such as the injection of morpholino oligonucleotides (Nasevicius and Ekker 2000), it will be possible to assess further the redundant and nonoverlapping functions of particular ANXs.

METHODS

Zebrafish

Methods for breeding and raising zebrafish were followed as described (Westerfield 1995). Embryos were obtained from natural matings of wild-type (Oregon, AB) fish and staged according to criteria previously outlined (Kimmel et al. 1995) and by hpf.

Cloning of Zebrafish *anx* Genes

PCR was used to amplify a 560-bp fragment of *Xenopus laevis anx*2 from a random primed tadpole library (gift of D. Brown, Carnegie Institution of Washington, Maryland). Primer sequences were 5′-GAGCTGAAGG CTTCAATG-3′ (forward) and 5′-GTCTAACTCACTTCGTGAAAC-3′ (reverse). A ^{32}P-labeled DNA probe, prepared by random priming of the gel-purified amplification product (Prime-It II; Stratagene), was used to screen a zebrafish postsomite stage cDNA library (gift of D. Grunwald, University of Utah Medical School, Utah) at low stringency (Sambrook et al. 1989). The protein sequences of the four zebrafish ANXs obtained from this screen were used for BLAST searches (Altschul et al. 1994) of >73,000 zebrafish EST sequences generated by the Zebrafish Genome Resources Project. The 212 *anx* EST sequences identified were clustered by using AssemblyLIGN software (Oxford Molecular Group). From this analysis, some unique clones were obtained commercially (Research Genetics) for complete DNA sequencing.

Seven additional *anx* clones were identified from the EST analysis. Two potential cloning artifacts were observed in commercially obtained clones. In the case of *anx2b* (clone fb57f04), the 5′ end was disrupted by a repetitive element. The correct missing 5′ sequence was obtained by using RACE (Frohman et al. 1988). The primer sequences were 5′-CTCTTTATTGCGAGAACACACCAT-3′, 5′-CATTCAACTAGT GTGAGGAAGG-3′, and 5′-CTCTCTCCCCTCCATAACTCA-3′.

The commercially obtained *anx13* clone (fb40a08) contained a shorter-than-expected open reading frame that appeared to be the result of a frame-shift mutation. To determine the correct *anx13* sequence, PCR was used to amplify a fragment from genomic DNA to find if it contained the frame shift (primer sequences, 5′-GGAGCCGGAACCGAT GAAGAC-3′ and 5′-GGAGGCGCTTG AAATCGCCTCCG-3′). After PCR, the fragment was gel purified and directly sequenced to reveal that the *anx13* frame-shift mutation was a cloning artifact.

Sequences of all zebrafish *anx* genes described in this paper have been deposited in GenBank. The accession nos. are as follows: *anx1a*, AY178793; *anx1b*, AY178794; *anx1c*, AY178795; *anx2a*, AY178796; *anx2b*, AY178797; *anx4*,

Table 2. Mapping Primers

Gene	Primer 1 5′ → 3′	Primer 2 5′ → 3′	Linkage group	Flanking markers		Distance from marker 1 cR (LOD)
				Marker 1	Marker 2	
anx1a	—	—	5	Z20915	Z21461	0.4 (>10)[a]
anx1b	CTCCCCTGGATTTTGAAACAT	CAGAAGAAAGGCAAACAGG	5	Z23067	*coe2*	4 (17.3)
anx1b	ACAACGAGATCAAAGCCAT	CCTCCAGCAGCTCCCCATA	5	Z23067	*coe2*	2 (15.9)
anx1c	GCTCTGTTTGAGGCAGGAGAG	CAGGCAGTCTTCAAGGTGTCCAC	5	Z23067	*coe2*	4.3 (14.3)
anx1c	GCTCTGTTTGAGGCAGGAGAG	AACCATCTTTGCTTAATTGGC	5	Z23067	*coe2*	4.5 (14.7)
anx2a	GTTCAGTGCTTTGAAAACAAACAGC TGTATTTCGCC	GGACACCATGATCCGGGTCAGCAC	25	*mariposa*	Z15401	10 (15.7)
anx2b	GTGTGAAAGACAAGATAATAACC	TGAAATTGTCTGGTGCAGAGATC	7	Z20853	Z11119	13 (15.4)
anx4	GAACATGACAAGAGTCTTGAAGAC	CTTTGCATCCTGGACAGCCTGAG	10	Z14193	Z6992	2 (19.0)
anx5	CTGAATCATTTTGTGCAGGG	GGGGCAGGCACTGACGATCAGACA	1	Z1463	Z7287	10 (14.4)
anx6	GCACGGACTGATGAACATGCG	CTGTGCCAGTGAGATCAGG	14	Z6674	Z3984	40 (13.2)
anx11a	GTGTTTAATGAGTACCAGCACATG	GACAGCCAGCATGCCGCTCTC	13	Z13682	Z9049	35 (12.1)
anx11b	GTGACTGAAGAGCAGGAGG	GCAAAGTATTTCTTGATTTCTC	12	Z4634	Z8254	5 (17.9)
anx13	GGAGCCGGAACCGATGAAGAC	GGAGGCGCTTGAAATCGCCTCCG	24	Z5413	Z23011	21 (11.4)

One centiray (cR) is equivalent to approximately 148 kilobases (Hukriede *et al.* 1999).
[a]An EST (fa05d11) identical to *anx1a* was previously mapped (Hukriede *et al.* 1999).

AY178798; *anx5*, AY178799; *anx6*, AY178800; *anx11a*, AY178801; *anx11b*, AY178802; and *anx13*, AY178803.

anx Gene Evolution

A phylogenetic trees showing the evolutionary relationship of the *anx* genes was produced using MacVector software (Accelrys). The final tree was determined by using UPGMA with ties resolved randomly by using 1000 bootstrap replications. Percentages represent the occurrence of the nodes. Trees were calculated from comparisons of the first 73–83 amino acids of the first ANX repeat.

Mapping and Syntenic Analysis

Zebrafish *anxs* were mapped using the LN54 Radiation Hybrid Panel as previously described (Hukriede et al. 1999). Primers for each gene are noted in Table 2. To determine syntenic relationships between zebrafish and human genomes, mapped zebrafish genes flanking a particular zebrafish *anx* gene were identified (maps used were Mother of Pearl Meiotic Map, GAT Meiotic Map, LN54 Radiation Hybrid Map; for map data, see http://zfin.org/cgi-bin/webdriver?Mlval=aa-refcrosslist.apg). The protein sequences of the flanking genes were used to identify human orthologs by BLAST searches. The chromosomal locations of human orthologs were determined by searching either the Human Gene Map99 Project or the Human Gene Database.

To confirm that the mapping of *anx1b* and *anx1c* to the same locus was not due to a PCR artifact (primers for one paralog actually amplify the other paralog), two sets of primers were used for each gene (Table 1), in which one set was designed in a region of the 3′UTR that was not similar between the sibling genes. Furthermore, a number of PCR products from the mapping reactions were cut from the mapping gel and directly sequenced, confirming that primers for *anx1b* were not amplifying *anx1c* and vice versa (data not shown).

Northern Analysis

For some *anx* genes (*anx1a*, *anx2a*, *anx5*, and *anx11a*), mRNA levels were detected by Northern analysis of total RNA (Sambrook et al. 1989) using a ^{32}P-labeled *anx* probe prepared by random priming of gel-purified zebrafish *anx* cDNAs (Prime-It II; Stratagene) and compared with expression observed with RNA in situ hybridization.

RNA In Situ Hybridization

In situ hybridization for *anx* expression was carried out as previously described (Thisse et al. 1993). Digoxigenin-labeled RNA probes synthesized for each gene were hybridized to embryos or larvae at 50% epiboly, 100% epiboly, tail bud, 1 somite, 5 somites, 15 somites, 20 somites, 24 hpf, 48 hpf, and 72 hpf. For double-labeled in situ hybridizations, probes were synthesized with either digoxigenin- or fluorescein-conjugated UTP and detected as previously described (Sagerstrom et al. 1996). After visualization, some embryos older than 24 h were refixed in 4% paraformaldehyde and sectioned as described (Westerfield, 1995).

ACKNOWLEDGMENTS

S.A.F was supported by an NRSA and Barbara McClintock Fellowship (Carnegie Institution); M.E.H., by a Pew's Scholar's Award. We also appreciated the helpful comments provided by Dr. John Dedman.

The publication costs of this article were defrayed in part by payment of page charges. This article must therefore be hereby marked "advertisement" in accordance with 18 USC section 1734 solely to indicate this fact.

REFFERENCES

Altschul, S., Boguski, M., Gish, W., and Wootton, J. 1994. Issues in searching molecular sequence databases. *Nat. Genet.* **6:** 119–129.

Amores, A., Force, A., Yan, Y., Joly, L., Amemiya, C., Fritz, A., Ho, R., Langeland, J., Prince, V., Wang, Y., et al. 1998. Zebrafish hox clusters and vertebrate genome evolution. *Science* **282:** 1711–1714.

Aparicio, S. 1998. Exploding vertebrate genomes. *Nat. Genet.* **18:** 301–303.

Bandorowicz-Pikula, J. and Pikula, S. 1998. Annexins and ATP in membrane traffic: A comparison with membrane fusion machinery. *Acta Biochim. Pol.* **45:** 721–733.

Bastian, B., van der Piepen, U., Romisch, J., Paques, E., and Brocker, E. 1993. Localization of annexins in normal and diseased human skin. *J. Dermatol. Sci.* **6:** 225–234.

Bonfils, C., Greenwood, M., and Tsang, A. 1994. Expression and characterization of a *Dictyostelium discoideum* annexin. *Mol. Cell. Biochem.* **139:** 159–166.

Brugge, J.S. 1986. The p35/p36 substrates of protein-tyrosine kinases as inhibitors of phospholipase A2. *Cell* **46:** 149–150.

Creutz, C.E. 1981. *cis*-Unsaturated fatty acids induce the fusion of chromaffin granules aggregated by synexin. *J. Cell. Biol.* **91:** 247–256.

Creutz, C.E., Snyder, S.L., Daigle, S.N., and Redick, J. 1996. Identification, localization, and functional implications of an abundant nematode annexin. *J. Cell. Biol.* **132:** 1079–1092.

Croxtal, J.D., Newman, S.P., Choudhury, Q., and Flower, R.J. 1996. The concerted regulation of cPLA2, COX2, and lipocortin 1 expression by IL-1β in A549 cells. *Biochem. Biophys. Res. Commun.* **220:** 491–495.

Davidson, F.F., Dennis, E.A., Powell, M., and Glenney Jr., J.R. 1987. Inhibition of phospholipase A2 by "lipocortins" and calpactins: An effect of binding to substrate phospholipids. *J. Biol. Chem.* **262:** 1698–1705.

Davidson, F.F., Lister, M.D., and Dennis, E.A. 1990. Binding and inhibition studies on lipocortins using phosphatidylcholine vesicles and phospholipase A2 from snake venom, pancreas, and a macrophage-like cell line. *J. Biol. Chem.* **265:** 5602–5609.

de Coupade, C., Gillet, R., Bennoun, M., Briand, P., Russo-Marie, F., and Solito, E. 2000. Annexin 1 expression and phosphorylation are upregulated during liver regeneration and transformation in antithrombin III SV40 T large antigen transgenic mice. *Hepatology* **31:** 371–380.

Donnelly, S. and Moss, S. 1997. Annexins in the secretory pathway. *Cell. Mol. Life Sci.* **53:** 533–538.

Dreier, R., Schmid, K., Gerke, V., and Riehemann, K. 1998. Differential expression of annexins I, II and IV in human tissues: An immunohistochemical study. *Histochem. Cell. Biol.* **110:** 137–148.

Drummond, I., Majumdar, A., Hentschel, H., Elger, M., Solnica, K.L., Schier, A., Neuhauss, S., Stemple, D., Zwartkruis, F., Rangini, Z., et al. 1998. Early development of the zebrafish pronephros and analysis of mutations affecting pronephric function. *Development* **125:** 4655–4667.

Emans, N., Gorvel, J.P., Walter, C., Gerke, V., Kellner, R., Griffiths, G., and Gruenberg, J. 1993. Annexin II is a major component of fusogenic endosomal vesicles. *J. Cell. Biol.* **120:** 1357–1369.

Fiedler, K. and Simons, K. 1995. Annexin homologues in *Giardia lamblia*. *Trends Biochem. Sci.* **20:** 177–178.

Force, A., Lynch, M., Pickett, F., Amores, A., Yan, Y., and Postlethwait, J. 1999. Preservation of duplicate genes by complementary, degenerative mutations. *Genetics* **151:** 1531–1545.

Frohman, M., Dush, M., and Martin, G. 1988. Rapid production of full-length cDNAs from rare transcripts: Amplification using a single gene-specific oligonucleotide primer. *Proc. Natl. Acad. Sci.* **85:** 8998–9002.

Gerke, V. and Moss, S. 1997. Annexins and membrane dynamics. *Biochim. Biophys. Acta* **1357:** 129–154.

Glenney Jr., J.R. 1985. Phosphorylation of p36 in vitro with pp60src: Regulation by Ca^{2+} and phospholipid. *FEBS Lett.* **192:** 79–82.

Halpern, M.E., Ho, R.K., Walker, C., and Kimmel, C.B. 1993. Induction of muscle pioneers and floor plate is distinguished by the zebrafish no tail mutation. *Cell* **75:** 99–111.

Herbomel, P., Thisse, B., and Thisse, C. 1999. Ontogeny and behaviour of early macrophages in the zebrafish embryo. *Development* **126:** 3735–3745.

Huang, K.S., Wallner, B.P., Mattaliano, R.J., Tizard, R., and Burne, C. 1986. Two human 35-kd inhibitors of phospholipase A2 are

related to substrates of pp60v-src and of the epidermal growth factor receptor/kinase. *Cell* **46:** 191–199.
Hukriede, N., Joly, L., Tsang, M., Miles, J., Tellis, P., Epstein, J., Barbazuk, W., Li, F., Paw, B., Postlethwait, J., et al. 1999. Radiation hybrid mapping of the zebrafish genome. *Proc. Natl. Acad. Sci.* **96:** 9745–9750.
Johnston, P.A., Perin, M.S., Reynolds, G.A., Wasserman, S.A., and Sudhof, T.C. 1990. Two novel annexins from *Drosophila melanogaster*: Cloning, characterization, and differential expression in development. *J. Biol. Chem.* **265:** 11382–11388.
Kaetzel, M., Chan, H., Dubinsky, W., Dedman, J., and Nelson, D. 1994. A role for annexin IV in epithelial cell function: Inhibition of calcium-activated chloride conductance. *J. Biol. Chem.* **269:** 5297–5302.
Kim, K.M., Kim, D.K., Park, Y.M., Kim, C.K., and Na, D.S. 1994. Annexin-I inhibits phospholipase A2 by specific interaction, not by substrate depletion. *FEBS Lett.* **343:** 251–255.
Kimmel, C., Ballard, W., Kimmel, S., Ullmann, B., and Schilling, T. 1995. Stages of embryonic development of the zebrafish. *Dev. Dyn.* **203:** 253–310.
Kobayashi, T., Gu, F., and Gruenberg, J. 1998. Lipids, lipid domains and lipid-protein interactions in endocytic membrane traffic. *Semin. Cell. Dev. Biol.* **9:** 517–526.
Konig, J., Prenen, J., Nilius, B., and Gerke, V. 1998. The annexin II-p11 complex is involved in regulated exocytosis in bovine pulmonary artery endothelial cells. *J. Biol. Chem.* **273:** 19679–19684.
Ma, A. and Ozers, L. 1996. Annexins I and II show differences in subcellular localization and differentiation-related changes in human epidermal keratinocytes. *Arch. Dermatol. Res.* **288:** 596–603.
Massey, H.D., Mayran, N., and Maroux, S. 1998. Polarized localizations of annexins I, II, VI and XIII in epithelial cells of intestinal, hepatic and pancreatic tissues. *J. Cell. Sci.* **111:** 3007–3015.
Meyer, A. and Schartl, M. 1999. Gene and genome duplications in vertebrates: The one-to-four (-to-eight in fish) rule and the evolution of novel gene functions. *Curr. Opin. Cell. Biol.* **11:** 699–704.
Minin, A.A., Zemskov, E.A., and Khaidarova, N.V. 1998. Protein kinase C and casein kinase 2 phosphorylate in vitro proteins of the annexin family from eggs of loach *Misgurnus fossilis*. *Biochemistry (Mosc.)* **63:** 1074–1077.
Mira, J.P., Dubois, T., Oudinet, J.P., Lukowski, S., Russo-Marie, F., and Geny, B. 1997. Inhibition of cytosolic phospholipase A2 by annexin V in differentiated permeabilized HL-60 cells: Evidence of crucial importance of domain I type II Ca^{2+}-binding site in the mechanism of inhibition. *J. Biol. Chem.* **272:** 10474–10482.
Morgan, R.O. and Fernandez, M.P. 1997. Annexin gene structures and molecular evolutionary genetics. *Cell. Mol. Life Sci.* **53:** 508–515.
Morgan, R.O. and Pilar Fernandez, M. 1997. Distinct annexin subfamilies in plants and protists diverged prior to animal annexins and from a common ancestor. *J. Mol. Evol.* **44:** 178–188.
Morgan, R.O., Jenkins, N.A., Gilbert, D.J., Copeland, N.G., Balsara, B.R., Testa, J.R., and Fernandez, M.P. 1999. Novel human and mouse annexin A10 are linked to the genome duplications during early chordate evolution. *Genomics* **60:** 40–49.
Moss, S. 1992, The annexins. In: *The annexins* (ed. S.E. Moss), pp. 1–10. Portland Press, Chapel Hill, NC.
Munz, B., Gerke, V., Gillitzer, R., and Werner, S. 1997. Differential expression of the calpactin I subunits annexin II and p11 in cultured keratinocytes and during wound repair. *J. Invest. Dermatol.* **108:** 307–312.
Nasevicius, A. and Ekker, S.C. 2000. Effective targeted gene "knockdown" in zebrafish. *Nat. Genet.* **26:** 216–220.
Nilius, B., Gerke, V., Prenen, J., Szucs, G., Heinke, S., Weber, K., and Droogmans, G. 1996. Annexin II modulates volume-activated chloride currents in vascular endothelial cells. *J. Biol. Chem.* **271:** 30631–30636.
Osterloh, D., Wittbrodt, J., and Gerke, V. 1998. Characterization and developmentally regulated expression of four annexins in the killifish medaka. *DNA Cell Biol.* **17:** 835–847.
Postlethwait, J., Yan, Y., Gates, M., Horne, S., Amores, A., Brownlie, A., Donovan, A., Egan, E., Force, A., Gong, Z., et al. 1998. Vertebrate genome evolution and the zebrafish gene map. *Nat. Genet.* **18:** 345–349.
Postlethwait, J., Amores, A., Force, A., and Yan, Y. 1999. The zebrafish genome. *Methods Cell. Biol.* **60:** 149–163.
Prince, V.E., Joly, L., Ekker, M., and Ho, R.K. 1998. Zebrafish hox genes: Genomic organization and modified colinear expression patterns in the trunk. *Development* **125:** 407–420.
Rajarao, S.J., Canfield, V.A., Mohideen, M.A., Yan, Y.L., Postlethwait, J.H., Cheng, K.C., and Levenson, R. 2001. The repertoire of Na,K-ATPase α and β subunit genes expressed in the zebrafish, *Danio rerio*. *Genome Res.* **11:** 1211–1220.
Raynor, C.M., Wright, J.F., Waisman, D.M., and Pryzdial, E.L. 1999. Annexin II enhances cytomegalovirus binding and fusion to phospholipid membranes. *Biochemistry* **38:** 5089–5095.
Sagerstrom, C., Grinbalt, Y., and Sive, H. 1996. Anteroposterior patterning in the zebrafish, *Danio rerio*: An explant assay reveals inductive and suppressive cell interactions. *Development* **122:** 1873–1883.
Sambrook, J., Fritsch, E., and Maniatis, T., 1989. *Molecular cloning: A laboratory manual*. Cold Spring Harbor Press, Cold Spring Harbor, NY.
Schlaepfer, D.D., Fisher, D.A., Brandt, M.E., Bode, H.R., Jones, J.M., and Haigler, H.T. 1992. Identification of a novel annexin in *Hydra vulgaris*: Characterization, cDNA cloning, and protein kinase C phosphorylation of annexin XII. *J. Biol. Chem.* **267:** 9529–9539.
Schmitz-Peiffer, C., Browne, C.L., Walker, J.H., and Biden, T.J. 1998. Activated protein kinase C α associates with annexin VI from skeletal muscle. *Biochem. J.* **330:** 675–681.
Seaton, B. 1996. *Annexins: Molecular structure to cellular function*. R.G. Landes Company, Austin, TX.
Smallwood, M.F., Gurr, S.J., Choudhari, U., and Bowles, D.J. 1990a. Characterization of plant annexin gene expression. *Biochem. Soc. Trans.* **18:** 1116.
Smallwood, M., Keen, J.N., and Bowles, D.J. 1990b. Purification and partial sequence analysis of plant annexins. *Biochem. J.* **270:** 157–161.
Smith, P. and Moss, S. 1994. Structural evolution of the annexin supergene family. *Trends Genet.* **10:** 241–246.
Thisse, C., Thisse, B., Schilling, T., and Postlethwait, J. 1993. Structure of the zebrafish *snail1* gene and its expression in wild-type, spadetail and no tail mutant embryos. *Development* **119:** 1203–1215.
Tokumitsu, H., Mizutani, A., Minami, H., Kobayashi, R., and Hidaka, H. 1992. A calcyclin-associated protein is a newly identified member of the Ca^{2+}/phospholipid-binding proteins, annexin family. *J. Biol. Chem.* **267:** 8919–8924.
Wagner, A. 2000. The role of population size, pleiotropy and fitness effects of mutations in the evolution of overlapping gene functions. *Genetics* **154:** 1389–1401.
Weinberg, E.S., Allende, M.L., Kelly, C.S., Abdelhamid, A., Murakami, T., Andermann, P., Doerre, O.G., Grunwald, D.J., and Riggleman, B. 1996. Developmental regulation of zebrafish MyoD in wild-type, no tail and spadetail embryos. *Development* **122:** 271–280.
Westerfield, M., 1995. *The zebrafish book*. University of Oregon, Eugene, OR.

WEB SITE REFERENCES

http://zfin.org/cgi-bin/webdriver?Mlval=aa-refcrosslist.apg; Listing of zebrafish mapping panels.

Received May 30, 2002; accepted in revised form April 7, 2003.